

# Tinengotinib (TT-00420), a Novel Spectrum-Selective Small-Molecule Kinase Inhibitor, Is Highly Active Against Triple-Negative Breast Cancer

Peng Peng<sup>1</sup>, Xiaoyan Qiang<sup>1</sup>, Guoyu Li<sup>1</sup>, Lin Li<sup>1</sup>, Shumao Ni<sup>1</sup>, Qi Yu<sup>1</sup>, Laura Sourd<sup>2</sup>, Elisabetta Marangoni<sup>2</sup>, Chao Hu<sup>3</sup>, Dong Wang<sup>3</sup>, Di Wu<sup>1</sup>, and Frank Wu<sup>1</sup>



## ABSTRACT

Triple-negative breast cancer (TNBC) is a highly heterogeneous cancer lacking actionable targets. Using a phenotypic screen of TNBC cells, we discovered a novel multiple kinase inhibitor tinengotinib (TT-00420) that strongly inhibited Aurora A/B, FGFR1/2/3, VEGFRs, JAK1/2, and CSF1R in biochemical assays. Exposure to tinengotinib specifically inhibited proliferation across all subtypes of TNBC *in vitro* and *in vivo*, while leaving luminal breast cancer cells intact. Incubation of HCC1806 with tinengotinib led to dose-dependent downregulation of genes essential for TNBC cell growth and proliferation.

Studies revealed that the potential mechanism of action of tinengotinib involved, predominantly, inhibition of Aurora A or B kinase activity, while inhibition of other pathways contributed to suppression of potency and activity. *In vitro* treatment of TNBC cell lines or *in vivo* administration in a syngeneic model with tinengotinib resulted in up-regulation of *CXCL10* and *11* or diminished tumor-associated macrophage (TAM) infiltration. Tinengotinib represents a novel combinatorial inhibitory mechanism to treat TNBC. The phase I trial of tinengotinib was completed (ClinicalTrials.gov identifier: NCT03654547).

## Introduction

Triple-negative breast cancer (TNBC), defined as a cancer subtype lacking expression of estrogen receptor (ER), progesterone receptor (PR), and HER2, accounts for 15%–20% of all breast cancers (1). Owing to its highly heterogeneous and aggressive nature and the absence of well-defined molecular targets of the disease, TNBC presents a major challenge to effective cancer therapy (2, 3).

Application of multiple ‘omics’ technologies have revealed an unexpected level of heterogeneity in TNBC. Lehmann and colleagues identified six TNBC subtypes, including two basal-like-related subgroups [basal-like 1/2 (BL1/2)], two mesenchymal-related subgroups [mesenchymal (MES) and mesenchymal stem-like (MSL)], one immunomodulatory subgroup (IM) and one luminal androgen receptor (LAR) group (4). By interrogating both mRNA and DNA profiles, this molecular subtyping was further refined to four stable and reproducible subtypes (5, 6), which includes one LAR, one MES, one basal-like immunosuppressed (BLIS) and one IM subtype.

Because of the intrinsic heterogeneity and the lack of actionable targets, chemotherapy and surgery still remain the primary therapeutic options for patients with newly diagnosed TNBC (7), and only a handful of targeted therapies have been approved as second-line or last-line options for the treatment of patients with TNBC. Additional potentially druggable targets or pathways in different TNBC subtypes have been identified by molecular profiling efforts. Both Aurora A and B are upregulated in BL1 and BL2 subtypes (4). Several receptor tyrosine kinase (RTK) signaling pathways, namely EGFR, FGFR, VEGFR, are commonly hyperactivated in BL2, M, and MSL. The IM subtype is characterized by the elevation of JAK/STAT signaling. Collectively, combinatorially targeting proto-oncogenic genes represent a promising therapeutic option to treat TNBC (4–6).

To tackle the clinical challenge of TNBC, we proposed to design a new drug modality that simultaneously targets several features of TNBC. This effort led to the discovery of a multi-kinase inhibitor, tinengotinib, which is capable of pharmacologically targeting several prominent signaling pathways in TNBC. This combined strategy resulted in universal proliferation inhibition, reduced angiogenesis and epithelial-mesenchymal cells transition (EMT), and elevated immuno-oncologic response in *in vitro* and *in vivo* TNBC models. Taken together, tinengotinib represents a novel strategy to treat TNBC by regulating several cancer pathways concomitantly, and the data in this work warrants further clinical development in TNBC.

## Materials and Methods

### Chemicals and reagents

Tinengotinib (WO2018108079A1, example 6, compound 29) were synthesized by TransThera. For *in vitro* assays, compounds were dissolved in DMSO to be 10 mmol/L as stock, then diluted to yield a final DMSO concentration of 1%. For *in vivo* efficacy studies, tinengotinib was formulated in 0.5% Methylcellulose (MC), and orally administered 10 mL/kg in volume to individuals with indicated dosages.

<sup>1</sup>Department of Medicinal Chemistry, Pharmacology, Project Management, Drug Metabolism and Pharmacokinetics, TransThera Sciences (Nanjing), Inc., Nanjing, Jiangsu, P.R. China. <sup>2</sup>Translational Research Department, Institute Curie, PSL Research University, Paris, France. <sup>3</sup>State Key Laboratory of Southwestern Chinese Medicine Resources, School of Basic Medical Sciences, Chengdu University of Traditional Chinese Medicine, Chengdu, China.

P. Peng and X. Qiang contributed equally to this article.

**Corresponding Author:** Peng Peng, TransThera Sciences (Nanjing), Inc., Fl 3, Bld 9, Phase 2 Accelerator, Biotech and Pharmaceutical Valley, Jiangbei New Area, Nanjing, Jiangsu 210032, P.R. China. E-mail: peng\_peng@transtherabio.com

Mol Cancer Ther 2023;22:205–14

doi: 10.1158/1535-7163.MCT-22-0012

This open access article is distributed under the Creative Commons Attribution-NonCommercial-NoDerivatives 4.0 International (CC BY-NC-ND 4.0) license.

©2022 The Authors; Published by the American Association for Cancer Research

### Kinase assays

Study was performed by mobility shift assay, ADP-Glo luminescent assay, Lance Ultra assay or Latha screen assay according to internally standard operating procedures (SOP) with ATP concentration at  $K_m$ . Tinengotinib at 500 nmol/L was initially used to assess the inhibitory activity on prototypic human kinases, and then  $IC_{50}$  values were determined for those with high inhibitory rate, under a 3-fold dilution series of concentrations starting from 3  $\mu$ mol/L.

### In vitro assays

#### Cellular viability assay, real-time PCR, and Western blotting

Cells were commercially purchased from ATCC or Cobioer, followed with short tandem repeat (STR) authentication and mycoplasma test by One-step Quickcolor Mycoplasma Detection Kit (Yisemed). Cells within 20 passages were seeded into cell culture plates (Nunc) overnight prior to use. The following day, cultures were refreshed with media containing tinengotinib or vehicle DMSO.

For cellular viability assays, cell viability was determined by CellTiter-Glo Luminescent Cell Viability Assay (Promega) or Cell Counting Kit-8 (Beyotime). For combinatorial assays, inhibitors of different mechanisms were mixed and diluted equally or with a fixed working concentration of 500 nmol/L. After 72 or 144 hours, cell viability was measured according to manufacturer's instructions.

For real-time PCR studies, cells were collected with indicated treatment intervals for further RNA isolation and cDNA synthesis, following manufacturer's instructions for RNAeasy Plus Universal Mini Kit (Qiagen) and HiScript II Q Select RT SuperMix for RNA (Vazyme), respectively. Relative mRNA levels of tested genes were quantified on ABI QuantStudio 12K Flex (Thermo Fisher Scientific) by SYBR Green (Vazyme) and calculated with  $-\Delta\Delta C_t$  method by normalization to *Gapdh* as reference. Relevant primer information is listed in Supplementary Table S1.

For Western blotting, cell lysates were collected by RIPA (Beyotime) after treated as indicated, quantified with BCA Protein Quantification Kit (Beyotime), and detected by antibodies listed in Supplementary Table S2.

#### Cell-cycle analysis

Cells were treated with tinengotinib at varying concentrations for 24 hours. Cells were collected and prepared under the manufacturer's instructions using PI/RNase Staining Buffer (BD Biosciences), and further analyzed by flow cytometry on the FACSCanto II Cytometer (BD Biosciences).

#### Wound-healing assay

HCC1806 cells were seeded in 6-well plates and scratched to simulate a wound site, and then treated with tinengotinib or DMSO for 24 hours. Images were captured by a microscope CCD camera (OPTIKA).

### In vivo models

All procedures related to animal handling, care and the treatment were performed according to guidelines approved by the Institutional Animal Care and Use Committee (IACUC) following the guidance of the Association for Assessment and Accreditation of Laboratory Animal Care (AAALAC).

#### Subcutaneous xenograft models

Patient-derived xenografts (PDX) were established from TNBC patients following informed consent as previously described (8). Performance of the experimental protocol and maintenance of animal

housing were conducted in accordance with institutional guidelines as proposed by the French Ethics Committee (Agreement B75-05-18). The TNBC molecular subtypes of PDX were determined on the basis of gene expression data with TNBCtype software (9).

Female nude mice were used for *in vivo* xenograft studies. For HCC1806 xenograft model,  $1 \times 10^6$  cells were inoculated subcutaneously; for PDX models, TNBC tumor fragments of about 1  $cm^3$  were inoculated subcutaneously. Mice were dosed after mean tumor sized reached approximate 100  $mm^3$ . Tinengotinib or vehicle was orally administrated once daily as indicated.

Tumor growth was evaluated by measuring two perpendicular tumor diameters with calipers twice a week. Individual tumor volumes were calculated:  $V = a \times b^2/2$ , where "a" is the largest diameter, "b" is the smallest diameter. For each tumor, volumes were expressed in relation to the initial volume as relative tumor volume (RTV). Tumor growth inhibition (TGI) of treated tumors versus vehicle control was calculated as the ratio of the mean RTV in the treated group to the mean RTV in the vehicle group at the same time.

In PDX models, for each tumor the percent change in volume was calculated as  $(V_f - V_0/V_0)/100$ ,  $V_0$  being the initial volume (at the beginning of treatment) and  $V_f$  the final volume (at the end of treatment). A decrease in tumor volume of at least 50% was classified as regression, an increase in tumor volume of at least a 35% identified progressive disease and volumes changes between +35% and -50% were considered as stable disease (10, 11).

For pharmacokinetic/pharmacodynamic analysis purpose, at 0, 0.5, 1, 3, 7, 12, and 24 hours after the last dosing in HCC1806 model, the blood and tumor samples were collected for pharmacokinetic analysis. For IHC analysis, formalin-fixed paraffin-embedded (FFPE) HCC1806 tumors were stained by hematoxylin and related antibodies as listed in Supplementary Table S2.

#### Matrigel plug assay

Female nude mice were inoculated subcutaneously with 0.5 mL Growth Factor Reduced (GFR) BD Matrigel matrix containing 0.05% BSA with or without 200 ng/mL bFGF and 600 ng/mL VEGF as "Matrigel plug" and randomized ( $n = 6$  per group). Tinengotinib or nintedanib, a typical anti-angiogenesis tool compound, was orally administrated once daily as indicated. Day 7 postrandomization, the Matrigel plug of individual mice was collected for gross observation and hemoglobin analysis. Hemoglobin quantity was normalized by its corresponding Matrigel plug weight.

#### Subcutaneous syngeneic models

The antitumor activity of tinengotinib monotherapy was evaluated in syngeneic murine models bearing 4T1 (TNBC) or MC38 (colon tumor) in Balb/C and C57/BL6 immunocompetent mice, respectively, as well as in immunodeficient NU/NU nude mice. Excised lungs in MC38 studies were fixed with Bouin-Hollande fixative, followed with pulmonary metastatic nodules counting and analysis. For combinatorial therapy study, tinengotinib were dosed with or without mice anti-PD-L1 antibody in mice with syngeneic murine MC38 subcutaneous inoculation. Murine cells were inoculated subcutaneously, and mice were dosed after mean tumor sized reached around 100  $mm^3$ .

#### Statistical analysis

The data were represented as the mean  $\pm$  SEM as indicated. Statistical analyses were performed in ordinary one-way ANOVA for studies of more than two groups, and two-tailed Student *t* tests for TV in *in vivo* PDX studies with only two groups in Prism 8.0 (GraphPad Software).  $P < 0.05$  was defined as significant differences.

### Clinical trials

The phase I, first-in-human, dose escalation and expansion study of tinengotinib (NCT03654547) enrolled adult patients with advanced or metastatic solid tumors as previously reported (12). On the basis of the manageable safety profile and the preliminary efficacy, a phase Ib/II TNBC-focused trial was initiated in the United States (NCT04742959) and China. All trials have obtained written informed consent from the patients with none were excluded.

### Data availability

The data generated in this study are available within the article and its Supplementary Data files.

## Results

### Phenotype-based screening identifies tinengotinib as a candidate to treat TNBC

We performed a preliminary screen in two TNBC cell lines, MDA-MB-468 and BT-549, using a focused kinase inhibitor library. A published compound with the structure of 7,8 -disubstituted pyrazolo benzodiazepine, was identified as an initial hit (13). A series of proprietary derivatives with 2-chlorophenyl substituted pyrido [4,3-*e*][1,4] diazepine scaffold were designed and synthesized. Among them, the morpholine compound tinengotinib (Fig. 1A) exhibited potent and balanced activities against MDA-MB-468 and BT-549. Tinengotinib also demonstrated acceptable liver microsome stabilities and good *in vivo* pharmacokinetic profiles (Supplementary Table S3). Therefore, tinengotinib was subjected to further exploration.

In a panel of human breast cancer cell lines, tinengotinib showed selective inhibition against TNBC lines, but not luminal cell lines, while CDK4/6 inhibitor palbociclib was effective only against luminal cell lines (Fig. 1B). We profiled tinengotinib against a panel of human

protein kinases *in vitro*, covering the majority of prototypic kinases (Supplementary Table S4). As shown in Table 1, tinengotinib demonstrated a spectrum-selective multi-target kinase profile, potently inhibiting kinases related to mitosis (Aurora A/B), angiogenesis (FGFR1/2/3, VEGFRs), tumor cell proliferation, and immune activity (JAK1/2, CSF1R). In addition, tinengotinib demonstrated favorable physicochemical properties and good safety profile to support its further development (Supplementary Tables S3 and S5).

### Tinengotinib suppresses the expression of “Achilles cluster” genes essential for TNBC cell growth and proliferation

Previous studies have identified a collection of signaling molecules and transcription factors (TF) whose expression levels are specifically enriched in TNBC but not in other breast cancer types. This group of genes, designated as the “Achilles cluster” of TNBC, represents collective vulnerability among TNBC (14). EGFR is predominantly upregulated in TNBC. FOSL1, a Fos family TF, is highly enriched as enhancers of cellular activity and acts as a key regulator of TNBC proliferation and viability (15). Twist1 is a basic helix-loop-helix (bHLH) domain-containing transcription factor, and it plays a critical role in EMT and cancer cell migration and invasion (16). Snai2, also known as Slug, promotes aggressiveness and resistance to therapy by enhancing cancer cell stem-like and EMT properties in TNBC (17). FOXC1 transcription factor, associated with TNBC metastasis, is identified as a crucial regulator and prognostic biomarker of TNBC (18). MYC is a bHLH zipper (bHLHZ) motif-containing transcription factor. As a well-established proto-oncogene, its amplification is found in 60% of TNBC (19) and involved in cell proliferation, survival, cancer cell stem-like properties, and immune suppression (20). To interrogate the effects of tinengotinib on the expression of “Achilles cluster”, TNBC cells HCC1806 were incubated with tinengotinib, and RNA was isolated for quantitative PCR analyses.

**Figure 1.**

Tinengotinib is highly active as a multi-kinase inhibitor in the treatment of TNBC. **A**, Chemical structure of tinengotinib. **B**, Heatmap depicting cellular sensitivity of tinengotinib and Palbociclib in Luminal ( $n = 7$ ) and TNBC ( $n = 6$ ) breast cancer types. Cells were treated by indicated compounds for 72 hours (TNBC) or 144 hours (Luminal).  $IC_{50}$  values (nmol/L) are shown in each cell. Data for Palbociclib was taken from published literature (31). **C**, Gene expression regulation of tinengotinib on a panel of TNBC-related genes by RT-qPCR in HCC1806 cells with 18-hour treatment ( $n = 3$ ). Gene expression level is normalized to vehicle (1% DMSO) group.

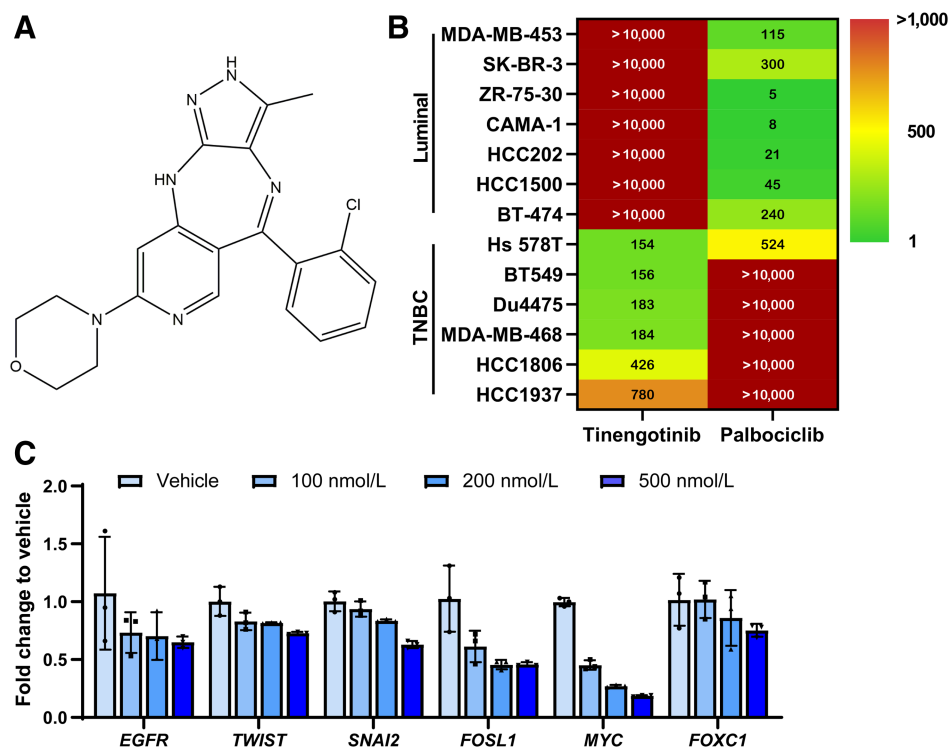


**Table 1.** Inhibitory activities of tinengotinib on human kinases.

Kinase	IC <sub>50</sub> /nmol/L	Kinase	IC <sub>50</sub> /nmol/L
Aurora A	1.2	KDR	2.5
Aurora B	3.3	VEGFR3	0.93
FGFR1	2.3	JAK1	15
FGFR2	1.5	JAK2	0.75
FGFR3	3.5	CSF1R	7.0
VEGFR1	2.4		

Incubation with tinengotinib led to downregulation of *EGFR*, *TWIST1*, *SNAI2*, *FOSL1*, *FOXCl*, and *MYC* (Fig. 1C). Taken together, tinengotinib represents a drug with a novel combinatorial inhibitory mechanism to for the treatment of TNBC.

#### The unique target combination profile of tinengotinib enables it to address combined oncogene addiction in TNBC

Codependency on multiple kinase networks has been proposed as an oncogenic advantage given the highly heterogeneous nature of TNBC. We wondered whether the multi-kinase inhibitory capacity of tinengotinib contributed to its unique target combination profile. A pharmacologic approach was taken to illustrate the mechanism of action of tinengotinib. In this study, selective Aurora A inhibitor (alisertib), selective Aurora B inhibitor (barasertib), pan-JAK inhibitor (tofacitinib), anti-angiogenetic inhibitor (lenvatinib), and EGFR inhibitor (erlotinib) were evaluated against a panel of five cancer cell lines representing five subtypes of TNBC. The IC<sub>50</sub> values of each drug alone, or of various combinations, were measured and compared with tinengotinib.

MDA-MB-468 cells, a BL1 subtype of TNBC, were sensitive to both alisertib and barasertib with an IC<sub>50</sub> comparable to that of tinengotinib. Combining either Aurora-selective inhibitor with tofacitinib or lenvatinib did not affect the IC<sub>50</sub> values (Table 2; Supplementary Fig. S1A). In a BL2-type cell line, HCC1806, none of the single agents produced an antiproliferative effect except tinengotinib. However, when combined with erlotinib, both Aurora-selective inhibitors demonstrated dramatically improved growth inhibitory effects, and the activity of the alisertib/erlotinib pair was >10 times more sensitive than that of barasertib/erlotinib pair, the latter of which could be improved with the addition of tofacitinib or lenvatinib. Combining alisertib with barasertib or the combination of tofacitinib, lenvatinib, and erlotinib or the combination of all five drugs did not further increase their inhibitory activity (Table 2; Supplementary Fig. S1B). In a representative MSL cell line Hs 578T, alisertib plus barasertib and a third drug gave rise to the most active inhibitory effect, while either drug combined with any other two drugs also demonstrated good potency (Table 2; Supplementary Fig. S1C). In the M subtype cell line, BT549, tinengotinib's antiproliferative capability was considered to rely solely on Aurora A inhibition; the alisertib/tofacitinib/lenvatinib combination exhibited the best activity (Table 2; Supplementary Fig. S1D). Finally, alisertib alone could effectively inhibit growth of the IM cell line Du4475, and this activity was not enhanced with additional drugs (Table 2; Supplementary Fig. S1E). In the combinatorial mechanism study, we demonstrated that inhibition of Aurora A or B lays the cornerstone for the pan-TNBC inhibitory effect of tinengotinib, while inhibition of angiogenesis, JAK family, or EGFR pathway further contributes to the potency and activity of tinengotinib.

#### Tinengotinib effectively blocks proliferation, angiogenesis, metastasis and epithelial-to-mesenchymal transition in tumor cells

Although combined pharmacologic inhibition recapitulated the anti-TNBC activities of tinengotinib, the biological consequences resulting from target engagement by tinengotinib was unclear, therefore a series of studies were performed to address this question.

#### Blockage of Aurora kinase pathway by tinengotinib

HCC1806 cells were synchronized at G<sub>2</sub>-M phase by the application of nocodazole, and treated with serial dilution of tinengotinib. The autophosphorylation of Aurora A/B and the phosphorylation of downstream signal Histone H3, direct substrate of Aurora B, were assayed to evaluate the antikinase activity of tinengotinib *in vitro*. As shown in Fig. 2A and S2, after 24 hours of treatment, the phosphorylation of Aurora pathway (p-Aurora A/B and p-Histone H3) were effectively inhibited. Interestingly, total protein levels of Aurora kinases were also slightly downregulated using the highest concentration of tinengotinib. The effect of Aurora kinase inhibition on cell cycle was determined by FACS analysis. After 24 hours of treatment, HCC1806 cells were arrested in G<sub>2</sub>-M phase in a dose-dependent manner, consistent with previous results of Aurora B inhibition (Fig. 2B; Supplementary Fig. S3). A similar cell-cycle arrest profile was also observed among other TNBC cell lines (Supplementary Fig. S3). In the HCC1806 tumor xenograft model, IHC staining of p-Histone H3 was performed and consistent with the *in vitro* observation, tinengotinib dose-dependently reduced p-Histone H3 level in tumors (Fig. 2C).

#### Blockage of EGFR pathway by tinengotinib

EGFR dependency was revealed pharmacologically in a number of TNBC cell lines (21). In the "Achilles" set, expression of *EGFR* was dose-dependently suppressed by tinengotinib. We wondered if suppression could be reflected at protein levels as well. In the HCC1806 cellular assay, phosphorylated EGFR diminished upon tinengotinib treatment, accompanied with according decrease of total EGFR protein level and consistent with the suppressed transcription of *EGFR* (Fig. 1C and Supplementary Fig. S4). Notably, in the same experiment, the protein levels of PTPN12, the tyrosine phosphatase as a tumor suppressor, downregulating the EGFR phosphorylation, whose targets include EGFR and HER2 but frequently compromised in TNBC (22), was not essentially increased across various concentrations of tinengotinib (Supplementary Fig. S4). Therefore, tinengotinib indirectly downregulated EGFR phosphorylation through the suppression of EGFR transcription but not PTPN12.

#### Blockage of VEGFR pathway by tinengotinib

Tinengotinib dramatically inhibited the cell viability at an IC<sub>50</sub> of 9.4 nmol/L (Supplementary Fig. S5). It blunted phosphorylation of VEGFR2 in HUVEC cells *in vitro* (Fig. 2D). To confirm the antiangiogenetic activity of tinengotinib, female Balb/C nude mice were injected subcutaneously with Matrigel matrix containing either 200 ng/mL bFGF and 600 ng/mL VEGF or 0.05% BSA. At the end point of the study, Matrigel implants were excised and homogenized for hemoglobin analysis. As shown in Fig. 2E, tinengotinib produced significant inhibition of angiogenesis in Matrigel plugs in mice. In the HCC1806 *in vivo* study, IHC staining of CD34, a known vascular endothelial cell biomarker, was performed on tumors. Similar trend on angiogenesis of tinengotinib was also observed with reduced CD34<sup>+</sup> vascular cells in tumors (Fig. 2F).

**Table 2.** Inhibition of Aurora kinases combined with other mechanisms contributes pan-TNBC suppression of tinengotinib.

Cell/ Subtype	IC <sub>50</sub> /nmol/L	Single					Combo of 2					Combo of 3					Combo of 4	Combo of 5	Tinengotinib	Critical Targets for TNBC							
		A	B	T	L	E	A			B		AB		AT	AL	BT	BL	TL			ABTL	ABTLE					
		T	L	E	T	L	E	T	L	E	L	E	E	L	E	E	E										
MDA-MB-468	BL1	73	18	#	#	#	57	65		15	18				72			17					47	AuKB/A			
HCC1806	BL2	#	#	#	#	#			384		5632	#	#	756	#	1002	607	#	1438	940	4654	#	560	240	AuKA+EGFR		
Hs 578T	MSL	#	#	#	#	#								178	274	279	6446	2035	432	589	890	908	#	197	170	167	AuKA+B
BT549	M	1666	#	#	#	#	525	1194		#	#				205			#						158	AuKA+JAK+VEGFR		
Du4475	IM	11	#	#	#	#	11	11		#	#				8			#						106	AuKA		

Note: TNBC cells were treated with combination of diverse inhibitors for different mechanisms related to tinengotinib for 72 hours to check the cell viability. Chosen inhibitors dosed equally in mol concentration in HCC1806 and Hs 578T, or fixed concentration of 500 nmol/mL for MDA-MB-468, BT549 and Du4475 (except for Aurora inhibitors with series dilution).

Abbreviations: **A**, alisertib, a selective Aurora A inhibitor; **B**, barasertib, a selective Aurora B inhibitor; **T**, tofacitinib citrate, a pan-JAK inhibitor; **L**, lenvatinib, antiangiogenesis by inhibiting VEGFR/FGFR; **E**, erlotinib, an EGFR inhibitor.

#IC<sub>50</sub> > 10,000 nmol/L.

**Blockage of JAK/STAT/IDO pathway by tinengotinib**

TNBC possesses a specific regulatory feedback loop incorporating increased IL6 and IL8 autocrine and paracrine signaling and the JAK/STAT signaling axis, to promote anchorage-independent growth, EMT transition, and resistance to apoptosis. The effects of tinengotinib on STAT3 phosphorylation in MDA-MB-231, an MSL TNBC cell line with elevated JAK/STAT3 activity, were evaluated by Western blot (Supplementary Fig. S6A). Tinengotinib exhibited dose-dependent inhibition on STAT3 phosphorylation. In HeLa cells, IFN $\gamma$ -stimulated IDO expression is mediated through the JAK/STAT3 pathway. The effect of tinengotinib was evaluated in rhIFN $\gamma$ -stimulated HeLa cells by Western blotting. Results indicated that tinengotinib dramatically inhibited cellular IDO expression (Supplementary Fig. S6B). Moreover, downstream genes in JAK/STAT pathway, including *CCND1*, *BCL2L1*, and *VEGFA*, were analyzed and suppressed expressions were observed in TNBC cells treated by tinengotinib (Supplementary Fig. S6C). Taken together, tinengotinib may modulate the proliferation, survival, invasiveness, and immune signaling in TNBC cells driven by dysregulated JAK/STAT3 pathway.

**Blockage of EMT by tinengotinib**

TNBC is characterized by enrichment of EMT markers and a high rate of distal metastases. Snai2 and Twist1, transcriptional factors directly regulating EMT, were downregulated by tinengotinib (Fig. 1C). In HCC1806 cells, the expression of N-cadherin (CDH2), a cell surface marker of active EMT, was downregulated with tinengotinib treatment (Supplementary Fig. S7A). Consistently with this finding is the demonstrating that tinengotinib dose-dependently blunted HCC1806 cancer cell migration in wound-healing assay (Supplementary Fig. S7B), and hampered lung metastasis nodules formation in MC38 *in vivo* mice models (Supplementary Fig. S7C).

**Tinengotinib is highly active in preclinical *in vivo* TNBC models**

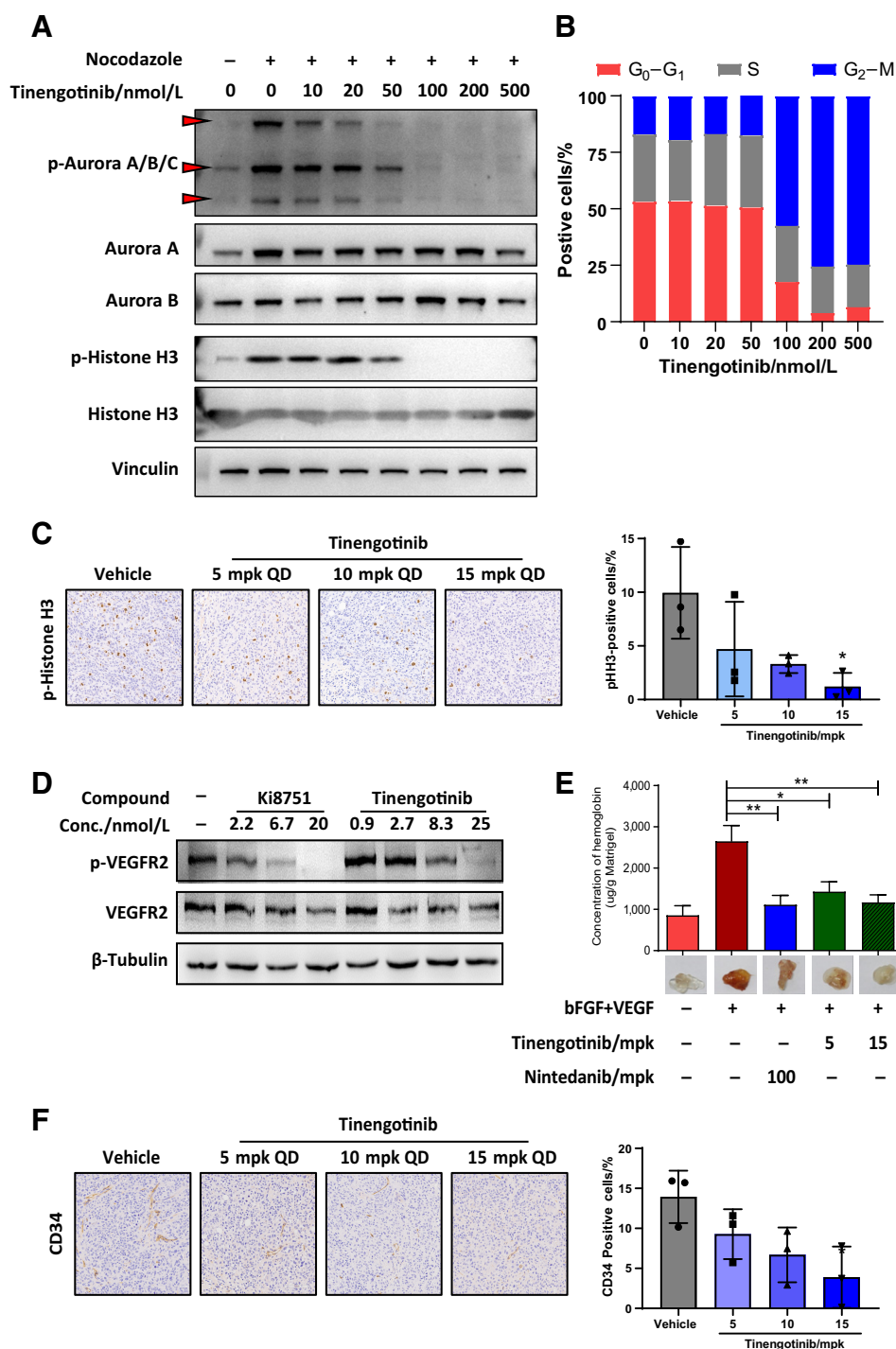
The *in vivo* anti-TNBC activities of tinengotinib were tested in a number of preclinical models. In the HCC1806 tumor xenograft model, tinengotinib displayed strong dose-dependent tumor growth inhibition (Fig. 3A). Plasma samples of all three treatment groups and tumor samples of 15 mg/kg group were collected, and the concentrations of tinengotinib were analyzed. As shown in Supplementary Table S6, both systematic C<sub>max</sub> and AUC<sub>last</sub> increased proportionally with dose escalation. After administration of 15 mg/kg, tinengotinib

quickly distributed to tumor sites, with slight accumulation and delayed peak concentration 7 hours postdosing. These data suggest good bioavailability and positive dose–efficacy correlation of tinengotinib in a tumor-bearing model.

To validate the effectiveness of tinengotinib in TNBC *in vivo*, we performed studies in 12 PDX models representing all molecular subtypes of TNBC (excepting IM; refs. 23, 24). Tinengotinib was administered orally at 15 mg/kg (MTD), and RTV and TGI were calculated. The detailed subtypes, genetic alterations and TGI are summarized in Supplementary Table S7. Tinengotinib demonstrated robust antitumor activity in all models tested, with TGI ranging from 61% to 99%. The tumor response of each animal dosed with tinengotinib was further analyzed according to RECIST 1.1 and illustrated in the waterfall plot. As shown in Fig. 3B, BL2/M/LAR and one of the UNS models exhibited significant tumor shrinkage after the monotherapy of tinengotinib, which met the partial response (PR) criteria.

In the mouse trial, BL1 and MSL were less sensitive to tinengotinib treatment. Paclitaxel is the current SOC for treatment-naïve TNBC patients. The MSL model HBCx-60 harbors a PI3KCA H1047R mutation. We further tested whether the combination with paclitaxel and BYL719 (PI3KCA inhibitor) in BL1 PDX HBCx-39 and MSL PDX HBCx-60, respectively, might synergize with tinengotinib. As shown in Fig. 3C and D, the antitumor activities of monotherapy with tinengotinib, paclitaxel, or BYL719 were consistent with previous studies. No obvious weight loss or other clinical abnormalities were observed during the treatment period (Supplementary Fig. S8). In both combination therapies, the antitumor growth effects were greatly enhanced as compared with single-agent groups, as tumor volume shrinkage was observed in multiple mice.

The anti-TNBC activity of tinengotinib was also evaluated in the drug-resistant setting using PDX BR1282. The study was carried out in a 2-phase design (Fig. 3E). In the first stage, tinengotinib and paclitaxel were administered to tumor-bearing mice according to the methods. Tinengotinib showed comparable antitumor activity (73% TGI) to Paclitaxel after 24 days of treatment (Fig. 3F). After initial response, tumors in the Paclitaxel group rapidly relapsed, the so-called TNBC paradox. The animals in the vehicle group and one mouse in the paclitaxel group were sacrificed according to the humane endpoints. In the second phase of the study, the remaining mice in the paclitaxel group whose tumor volumes reached 1,000 mm<sup>3</sup> were switched to tinengotinib. Switching paclitaxel to tinengotinib manifested dramatic TGI (Fig. 3G).



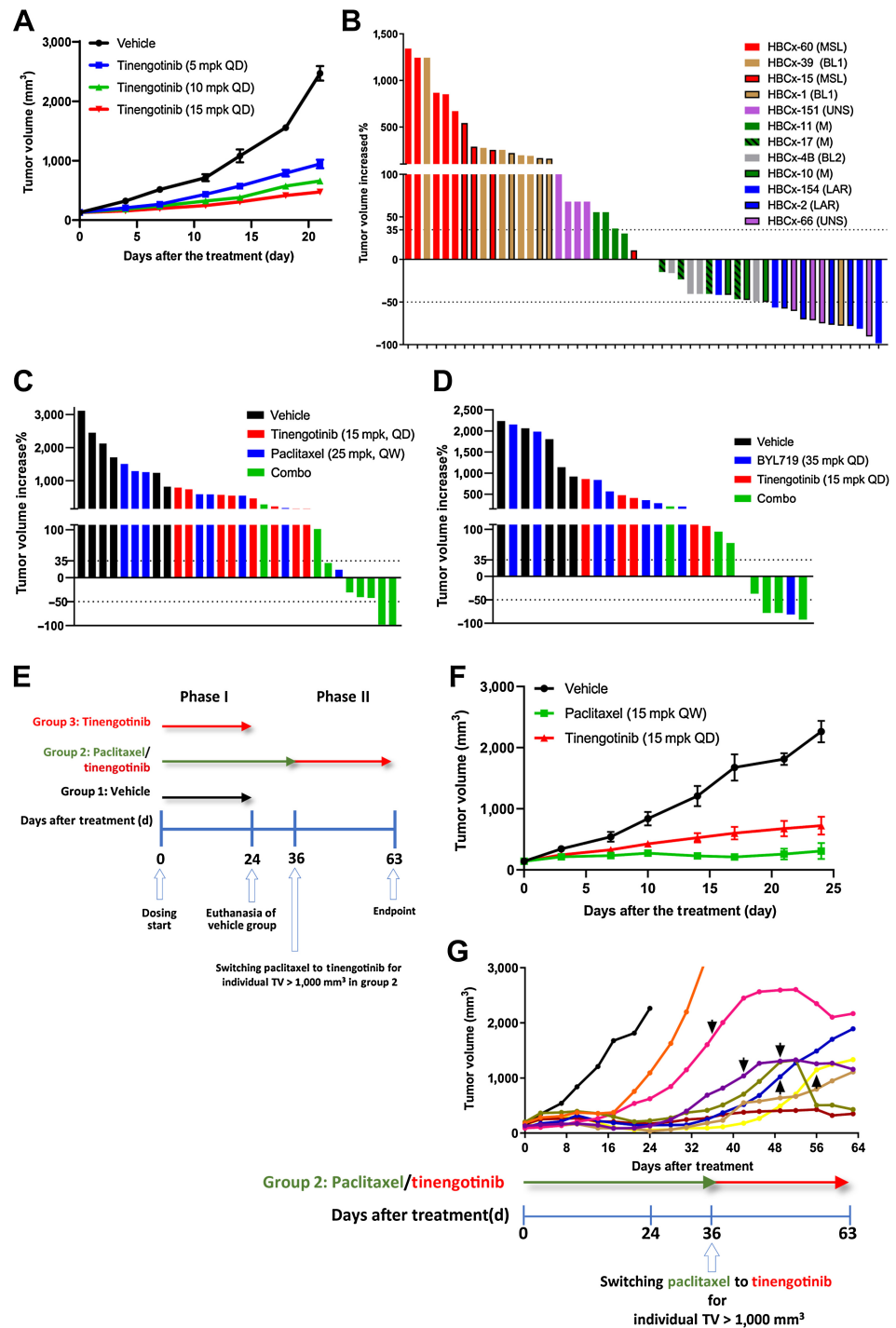
**Tinengotinib possesses robust immunomodulatory activity**

A recent paradigm shift has repositioned small-molecule kinase inhibitors as both targeted and immune modulators. We hypothesized that the target profile of tinengotinib may confer its immunomodulatory activity. To test this hypothesis, syngeneic murine 4T1 TNBC tumors were inoculated in immune-competent Balb/C mice, as well as the immuno-deficient NU/NU nude mice, to evaluate the antitumor activity of tinengotinib. Tinengotinib exhibited significant tumor growth inhibition in tumor-bearing NU/NU

nude mice, and this activity was greatly enhanced in immunocompetent Balb/C mice (Fig. 4A and B). This phenomenon was recapitulated in syngeneic murine MC38 colon tumor model (Supplementary Fig. S9A and S9B). The enhanced anti-tumor activities in immune-competent mice strongly suggested an immunomodulatory contribution of tinengotinib. This was further confirmed in a second study in MC38, a commonly used model in proof-of-concept study in combination therapy. When combined with PD-L1 blockade, a clinically approved treatment in TNBC,

**Figure 3.**

Tinengotinib is highly active in preclinical *in vivo* TNBC models. **A**, HCC1806 TNBC subcutaneous xenograft model was orally treated with tinengotinib or vehicle (0.5% MC) once daily as indicated. Tumor volumes are presented as geometric Mean  $\pm$  SEM ( $n = 8$ , except for 15 mpk which is of  $n = 21$  for pharmacokinetic blood collection). **B**, TNBC PDX models covering most of the TNBC subtypes (except for IM) were orally administered with 15 mg/kg tinengotinib or vehicle once daily and 5 days a week up to 4 weeks ( $n = 3-5$ ). The percent tumor volume change from baseline (tumor volume at the time of randomization) at the end of treatment is depicted, and each bar represents an individual xenograft. **C**, HBCx-39 TNBC PDX model was treated with monotherapy or combinatorial therapy of tinengotinib (5 days per week, orally) and paclitaxel (i.p.). The percent of tumor volume change from baseline is depicted, and each bar represents an individual xenograft ( $n = 6-8$ ). **D**, HBCx-60 TNBC PDX model (with *PIK3CA* mutated) was treated with monotherapy or combinatorial therapy of tinengotinib (5 days per week, PO) and BYL719 (5 days per week, orally). The percent of tumor volume change from baseline is depicted, and each bar represents an individual xenograft ( $n = 6-8$ ). BYL719 is a selective PI3K $\alpha$  inhibitor. **E-G**, BR1282 TNBC PDX model was administered as shown (**E**), together with tumor volume of each treatment (**F**; mean  $\pm$  SEM,  $n = 8$ ). After day 36 postrandomization, mice in paclitaxel group (group 2) switched to tinengotinib treatment once tumor volume reached, 1,000 mm<sup>3</sup>, as shown by the black arrows (**G**). Each colorful line represents an individual in group 2, while black line represents the mean tumor volume for vehicle group.



tinengotinib displayed further enhanced tumor growth inhibition (Supplementary Fig. S9C).

The immunomodulatory activity of tinengotinib may be attributed to its inhibitory effect on CSF1R which is expressed on tumor-associated macrophages (TAM). In the tumor microenvironment, TAMs play an important role in promoting immune suppression and accelerating tumor cell growth, survival, and metastasis. Upon the activation of the colony-stimulating factor 1 receptor (CSF1R) through the binding of macrophage colony stimulating

factor 1 (M-CSF), TAMs are predominantly polarized to a protumorigenic M2 phenotype (25). The effects of tinengotinib on CSF1R phosphorylation in CSF1R-overexpressed 293T cells were evaluated by Western blot, and the results showed that tinengotinib inhibited the phosphorylation of CSF1R in a dose-dependent manner (Supplementary Fig. S9D). The functional significance of this inhibition was further evaluated in human peripheral blood mononuclear cells (PBMC). The differentiation of PBMC to macrophage induced by 100 ng/mL of rhM-CSF was completely abolished by tinengotinib in

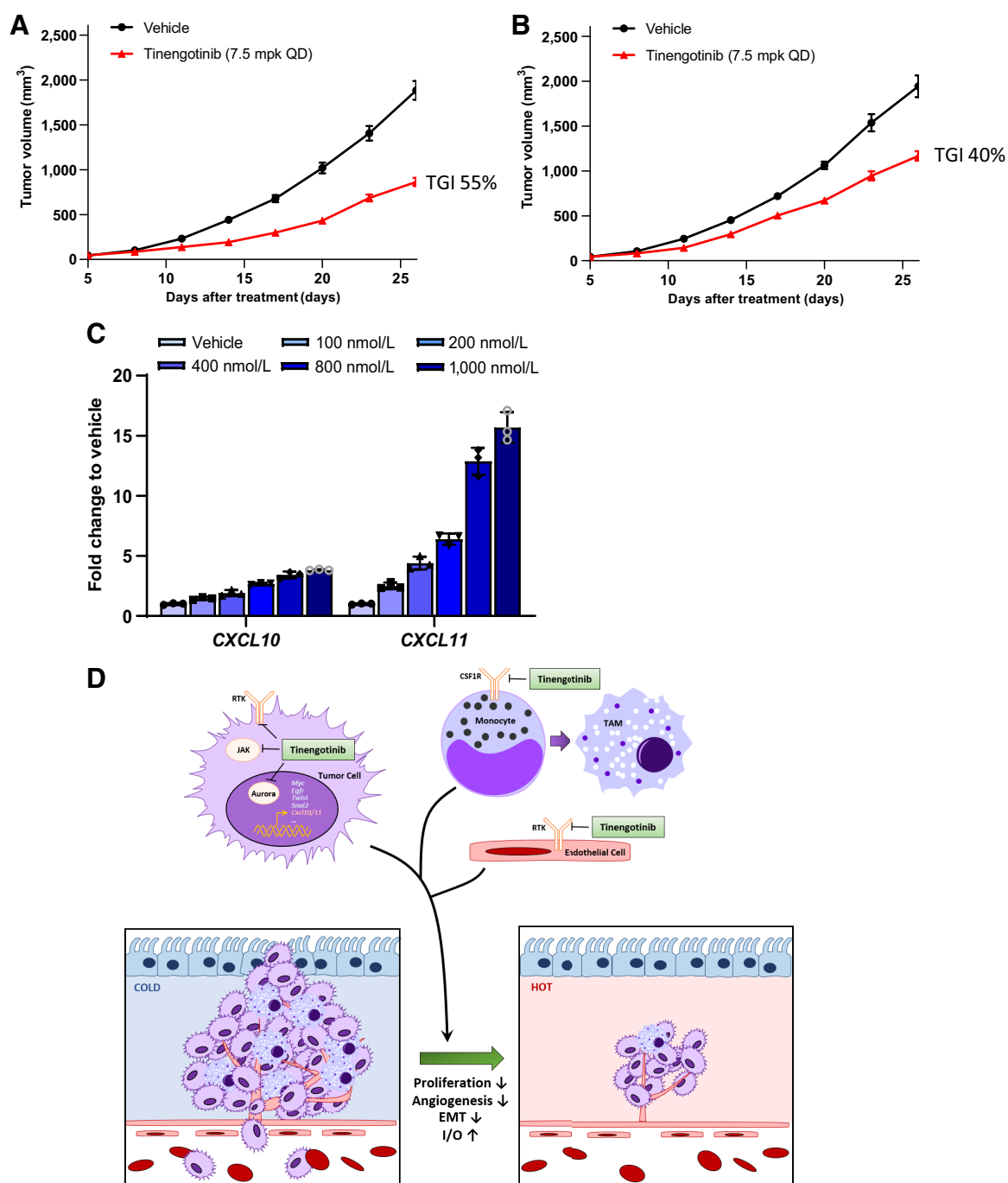


**Figure 4.** Tinengotinib possesses robust immuno-oncology activity. **A** and **B**, Tinengotinib possesses robust immuno-oncology activity. Murine TNBC cell line 4T1 cells were inoculated in immunocompetent Balb/C mice (**A**) and immunodeficient NU/NU nude mice (**B**) and orally treated with tinengotinib as indicated once daily. Tumor volume of each treatment was shown in the figures (mean ± SEM,  $n = 6$  or  $12$ ). **C**, Gene expression regulation of tinengotinib on tumor immunology phenotyping genes by RT-qPCR in murine TNBC cell line 4T1 with 24-hour treatment ( $n = 3$ ). Gene expression level is normalized to vehicle (1% DMSO) group. **D**, Schematic illustration of the possible molecular mechanism of tinengotinib in TNBC.

a concentration-dependent manner (Supplementary Fig. S9E). In the MC38 monotherapy study, tinengotinib treatment resulted in decreased infiltration of TAM in tumors (Supplementary Fig. S9F).

It has been reported that inhibition of Aurora kinase activates the expression of TH1-type chemokines in TNBC cells (26), and this mechanism might contribute to the ability of tinengotinib to modulate tumor microenvironment. Treatment of murine TNBC 4T1 cells and a

panel of human TNBC cells with tinengotinib clearly increased the expression of both TH1 chemokines *CXCL10* and *CXCL11* in a dose-dependent manner (Fig. 4C; Supplementary S9G). Taken together, tinengotinib is a novel kinase inhibitor in possession of multiple mechanisms of action against TNBC.

## Discussion

Many oncogenic driver mutations have been identified in cancers, and interception of druggable targets by small molecules or antibodies have profoundly transformed the cancer therapy landscape. However, in highly heterogeneous cancers, the lack of actionable targets and co-dependency on multiple pathways present a challenge to ad hoc drug development. In this study, we demonstrate the feasibility of using phenotypic screening to identify a spectrum-focused kinase inhibitor, tinengotinib with broad target specificity capable of intercepting multiple oncogenic pathways simultaneously. We revealed that the inhibition of Aurora kinases by tinengotinib is required for its pan-anti-TNBC activity, and the additional inhibitory effect on VEGFR/FGFR, JAK/STAT, and EGFR pathways, are sufficiently broad to cover all TNBC subtypes, regardless of known biomarkers, such as TP53 deficiency, RB loss, and BRCA mutations. Our discovery not only reconfirms the highly heterogeneous nature of TNBC, but also echoes the clinical challenge of using only target-selective intervention to treat heterogeneous cancers.

Mechanistically, we observed tumor reduction by tinengotinib via multiple combined pathways, although we believe that each engaged target may not contribute equivalently as exemplified by the reliance on Aurora inhibition in our combinatorial pharmacologic studies. Both Aurora A and B were pharmacologically targeted to inhibit the proliferation of cancer cells, but recent advances in Aurora biology have greatly enhanced our understating of their essential roles in cancer development and progression, in addition to their canonical functions in cell cycle control. In TP53-deficient, NRAS-driven and MYC-expressing hepatocellular carcinomas (HCC), MYC is stabilized through the interaction with Aurora A, and the disruption of MYC/Aurora A complex by conformation-changing Aurora A inhibitors to prevent the de novo formation of the complex results in MYC degradation and apoptosis of cancer cells (27). A reciprocal activation between Aurora B and MYC was also discovered in T cell acute lymphoblastic leukemia (T-ALL; ref. 28). In the recent report by Wang (26), treatment of TNBC cells with Aurora inhibitors up-regulates the expression of *CXCL10* and *11*, and transforms the tumor microenvironment from an immune-inhibitory to an immune-active state, mainly through perturbation of the Aurora A/STAT3 axis. Altogether, Aurora kinase elicits and maintains many hallmarks of cancer (29) by directly regulating several key players of oncogenic transformation.

The pleiotropic effects of tinengotinib may in part be attributable to its primary inhibitory effect on Aurora kinase. Tinengotinib may disrupt Aurora/MYC complex and destabilize MYC in TNBC, leading to a breakdown of MYC-regulated oncogenic programs (27). Tinengotinib also exerts direct antiproliferative and immunomodulatory effects through inhibition of Aurora in cell-cycle and Aurora/STAT3 pathways, respectively. Intriguingly, whether Aurora A or B or both participate in Aurora/MYC formation and the mechanism of tinengotinib to disassemble such a complex in TNBC are worthy of further investigation.

Numerous subtype-selective or pan-Aurora kinase inhibitors have entered clinical trials, but without exception, their clinical develop-

ments were halted due to the lack of efficacy. These results are consistent with our findings, in which Aurora inhibition is required, but not sufficient, to render the pan-TNBC antitumor activity of tinengotinib. As discussed above, pharmacologic inhibition of VEGFR, JAK/STAT, EGFR and CSF1R signaling pathways in tumor cells, endothelial cells and TAM, respectively, by tinengotinib leads to inhibition of proliferation, reversal of immune-suppression, and enhanced trafficking of effector T cells into tumor microenvironment (Fig. 4D). This is reminiscent of the “one-two punch” therapeutic strategy for the cancer cells (30), in which TNBC cells are induced to acquire vulnerability by Aurora inhibition, and that are subsequently targeted and killed by additional inhibitions. Thus, tinengotinib represents a rational strategy to treat TNBC by concomitantly targeting a number of cancer hallmarks including proliferation, angiogenesis, EMT, and immune-oncology through the inhibition on several prominent oncogenic pathways (Fig. 4D).

We have completed the phase I dose escalation study of tinengotinib in patients with advanced solid tumors (12). Tinengotinib was well tolerated across 7 cohorts evaluated, with good pharmacokinetic parameter compatible with orally once daily regimen. Promising clinical signals were observed in the 5 evaluable TNBC patients with 1 partial response (PR) and 2 stable disease (SD). Most importantly, in patients with TNBC who were well tolerated and benefited from tinengotinib, the drug exposure was in the efficacious range of pharmacokinetic/pharmacodynamic study. On the basis of the manageable safety profile and the preliminary efficacy, a phase Ib/II TNBC-focused trial was initiated in the United States (ClinicalTrials.gov identifier: NCT04742959) and China.

## Authors' Disclosures

P. Peng reports grants from Development Center for Medical Science & Technology National Health Commission of the People's Republic of China and grants from Jiangsu Provincial Department of Science and Technology during the conduct of the study; in addition, P. Peng has a patent for WO2018108079A1 issued to TransThera Sciences (Nanjing), Inc. and a patent for PCT/CN2022/091924 pending. X. Qiang reports grants from Development Center for Medical Science & Technology National Health Commission of the People's Republic of China and grants from Jiangsu Provincial Department of Science and Technology during the conduct of the study; in addition, X. Qiang has a patent for WO2018108079A1 issued to TransThera Sciences (Nanjing), Inc. and a patent for PCT/CN2022/091924 pending. G. Li reports grants from Development Center for Medical Science & Technology National Health Commission of the People's Republic of China and grants from Jiangsu Provincial Department of Science and Technology during the conduct of the study; in addition, G. Li has a patent for WO2018108079A1 issued to TransThera Sciences (Nanjing), Inc. and a patent for PCT/CN2022/091924 pending. L. Li reports grants from Development Center for Medical Science & Technology National Health Commission of the People's Republic of China and grants from Jiangsu Provincial Department of Science and Technology during the conduct of the study; in addition, L. Li has a patent for WO2018108079A1 issued to TransThera Sciences (Nanjing), Inc. and a patent for PCT/CN2022/091924 pending. S. Ni reports grants from Development Center for Medical Science & Technology National Health Commission of the People's Republic of China and grants from Jiangsu Provincial Department of Science and Technology during the conduct of the study; in addition, S. Ni has a patent for WO2018108079A1 issued to TransThera Sciences (Nanjing), Inc. and a patent for PCT/CN2022/091924 pending. Q. Yu reports grants from Development Center for Medical Science & Technology National Health Commission of the People's Republic of China and grants from Jiangsu Provincial Department of Science and Technology during the conduct of the study; in addition, Q. Yu has a patent for WO2018108079A1 issued to TransThera Sciences (Nanjing), Inc. and a patent for PCT/CN2022/091924 pending. E. Marangoni reports grants from TransThera Sciences during the conduct of the study. D. Wang reports grants from National Natural Science Foundation of China, grants from Science & Technology Department of Sichuan Province, and grants from Science and Technology Plan of Inner Mongolia Autonomous Region outside the submitted work. D. Wu reports grants from Development Center for Medical Science

& Technology National Health Commission of the People's Republic of China and grants from Jiangsu Provincial Department of Science and Technology during the conduct of the study; in addition, D. Wu has a patent for PCT/CN2022/091924 issued to TransThera Sciences (Nanjing), Inc. and a patent for PCT/CN2022/091924 pending. F. Wu reports grants from Development Center for Medical Science & Technology National Health Commission of the People's Republic of China and grants from Jiangsu Provincial Department of Science and Technology during the conduct of the study; in addition, F. Wu has a patent for WO2018108079A1 issued to TransThera Sciences (Nanjing), Inc. and a patent for PCT/CN2022/091924 pending. No disclosures were reported by the other authors.

## Authors' Contributions

**P. Peng:** Conceptualization, data curation, supervision, funding acquisition, investigation, methodology, writing—original draft. **X. Qiang:** Conceptualization, data curation, investigation, visualization, methodology, writing—original draft, project administration, writing—review and editing. **G. Li:** Data curation, methodology. **L. Li:** Methodology. **S. Ni:** Data curation, methodology. **Q. Yu:** Data curation, visualization, methodology, project administration, writing—review and editing. **L. Sourd:** Methodology. **E. Marangoni:** Data curation, visualization, methodology, writing—review and editing. **C. Hu:** Data curation, methodology. **D. Wang:**

Methodology. **D. Wu:** Funding acquisition, methodology. **F. Wu:** Conceptualization, supervision, funding acquisition, methodology.

## Acknowledgments

This work was financially supported by National Science and Technology Major Projects for “Major New Drugs Innovation and Development” (2019ZX09301-158) and Jiangsu Provincial Special Fund for “Transformation of Scientific and Technological Achievements” (BA2019057).

The publication costs of this article were defrayed in part by the payment of publication fees. Therefore, and solely to indicate this fact, this article is hereby marked “advertisement” in accordance with 18 USC section 1734.

## Note

Supplementary data for this article are available at Molecular Cancer Therapeutics Online (<http://mct.aacrjournals.org/>).

Received January 5, 2022; revised June 24, 2022; accepted October 7, 2022; published first October 12, 2022.

## References

- Perou CM, Sorlie T, Eisen MB, van de Rijn M, Jeffrey SS, Rees CA, et al. Molecular portraits of human breast tumours. *Nature* 2000;406:747–52.
- Carey L, Winer E, Viale G, Cameron D, Gianni L. Triple-negative breast cancer: disease entity or title of convenience? *Nat Rev Clin Oncol* 2010;7:683–92.
- Foulkes WD, Smith IE, Reis-Filho JS. Triple-negative breast cancer. *N Engl J Med* 2010;363:1938–48.
- Lehmann BD, Bauer JA, Chen X, Sanders ME, Chakravarthy AB, Shyr Y, et al. Identification of human triple-negative breast cancer subtypes and preclinical models for selection of targeted therapies. *J Clin Invest* 2011;121:2750–67.
- Burstein MD, Tsimelzon A, Poage GM, Covington KR, Contreras A, Fuqua SA, et al. Comprehensive genomic analysis identifies novel subtypes and targets of triple-negative breast cancer. *Clin Cancer Res* 2015;21:1688–98.
- Lehmann BD, Jovanović B, Chen X, Estrada MV, Johnson KN, Shyr Y, et al. Refinement of triple-negative breast cancer molecular subtypes: implications for neoadjuvant chemotherapy selection. *PLoS One* 2016;11:e0157368.
- Biomedtracker. Triple-negative breast cancer KOL. In: Biomedtracker, editor. US2019.
- Coussy F, de Koning L, Lavigne M, Bernard V, Ouine B, Boulai A, et al. A large collection of integrated genomically characterized patient-derived xenografts highlighting the heterogeneity of triple-negative breast cancer. *Int J Cancer* 2019; 145:1902–12.
- Chen X, Li J, Gray WH, Lehmann BD, Bauer JA, Shyr Y, et al. TNBCtype: a subtyping tool for triple-negative breast cancer. *Cancer Inform* 2012;11:147–56.
- Bertotti A, Migliardi G, Galimi F, Sassi F, Torti D, Isella C, et al. A molecularly annotated platform of patient-derived xenografts (“xenopatients”) identifies HER2 as an effective therapeutic target in cetuximab-resistant colorectal cancer. *Cancer Discov* 2011;1:508–23.
- Coussy F, El-Botty R, Château-Joubert S, Dahmani A, Montaudon E, Leboucher S, et al. BRCA1, SLC11, and RB1 loss predict response to topoisomerase I inhibitors in triple-negative breast cancers. *Sci Transl Med* 2020;12:eaa2625.
- Piha-Paul SA, Xu BH, Raghav KPS, Meric-Bernstam F, Janku F, Dumbrava EE, et al. First-in-human, phase I study of TT-00420, a multiple kinase inhibitor, as a single agent in advanced solid tumors. *J Clin Oncol* 2021;39 (15\_suppl):3090.
- Liu JJ, Higgins B, Ju G, Kolinsky K, Luk KC, Packman K, et al. Discovery of a highly potent, orally active mitosis/angiogenesis inhibitor r1530 for the treatment of solid tumors. *ACS Med Chem Lett* 2013;4:259–63.
- Franco HL, Nagari A, Malladi VS, Li W, Xi Y, Richardson D, et al. Enhancer transcription reveals subtype-specific gene expression programs controlling breast cancer pathogenesis. *Genome Res* 2018;28:159–70.
- Qin Q, Xu Y, He T, Qin C, Xu J. Normal and disease-related biological functions of Twist1 and underlying molecular mechanisms. *Cell Res* 2012;22:90–106.
- Majorini MT, Manenti G, Mano M, De Cecco L, Conti A, Pinciroli P, et al. cIAP1 regulates the EGFR/Snai2 axis in triple-negative breast cancer cells. *Cell Death Differ* 2018;25:2147–64.
- Ray PS, Wang J, Qu Y, Sim MS, Shamonki J, Bagaria SP, et al. FOXC1 is a potential prognostic biomarker with functional significance in basal-like breast cancer. *Cancer Res* 2010;70:3870–6.
- Horiuchi D, Kusdra L, Huskey NE, Chandriani S, Lenburg ME, Gonzalez-Angulo AM, et al. MYC pathway activation in triple-negative breast cancer is synthetic lethal with CDK inhibition. *J Exp Med* 2012;209:679–96.
- Foley S, Castell A, Kavanagh E, Synnott N, Duffy MJ. MYC as a therapeutic target for the treatment of triple-negative breast cancer. *J Clin Oncol* 2019;37:e12550.
- Fink LS, Beatty A, Devarajan K, Peri S, Peterson JR. Pharmacological profiling of kinase dependency in cell lines across triple-negative breast cancer subtypes. *Mol Cancer Ther* 2015;14:298–306.
- Sun T, Aceto N, Meerbrey KL, Kessler JD, Zhou C, Migliaccio I, et al. Activation of multiple proto-oncogenic tyrosine kinases in breast cancer via loss of the PTPN12 phosphatase. *Cell* 2011;144:703–18.
- Nair A, Chung HC, Sun T, Tyagi S, Dobrolecki LE, Dominguez-Vidana R, et al. Combinatorial inhibition of PTPN12-regulated receptors leads to a broadly effective therapeutic strategy in triple-negative breast cancer. *Nat Med* 2018;24: 505–11.
- Marangoni E, Vincent-Salomon A, Auger N, Degeorges A, Assayag F, de Cremoux P, et al. A new model of patient tumor-derived breast cancer xenografts for preclinical assays. *Clin Cancer Res* 2007;13:3989–98.
- Marangoni E, Laurent C, Coussy F, El-Botty R, Château-Joubert S, Servely JL, et al. Capecitabine efficacy is correlated with TYMP and RB1 expression in PDX established from triple-negative breast cancers. *Clin Cancer Res* 2018; 24:2605–15.
- Zhou Y, Shan S, Li ZB, Xin LJ, Pan DS, Yang QJ, et al. CS2164, a novel multi-target inhibitor against tumor angiogenesis, mitosis and chronic inflammation with anti-tumor potency. *Cancer Sci* 2017;108:469–77.
- Wang H, Li S, Wang Q, Jin Z, Shao W, Gao Y, et al. Tumor immunological phenotype signature-based high-throughput screening for the discovery of combination immunotherapy compounds. *Sci Adv* 2021;7:eabd7851.
- Dauch D, Rudalska R, Cossa G, Nault JC, Kang TW, Wuestefeld T, et al. A MYC-aurora kinase a protein complex represents an actionable drug target in p53-altered liver cancer. *Nat Med* 2016;22:744–53.
- Jiang J, Wang J, Yue M, Cai X, Wang T, Wu C, et al. Direct phosphorylation and stabilization of MYC by aurora B kinase promote T-cell leukemogenesis. *Cancer Cell* 2020;37:200–15.
- Hanahan D, Weinberg RA. Hallmarks of cancer: the next generation. *Cell* 2011; 144:646–74.
- Chi F, Liu J, Brady SW, Cosgrove PA, Nath A, McQuerry JA, et al. A ‘one-two punch’ therapy strategy to target chemoresistance in estrogen receptor positive breast cancer. *Transl Oncol* 2021;14:100946.
- Finn RS, Dering J, Conklin D, Kalous O, Cohen DJ, Desai AJ, et al. PD 0332991, a selective cyclin D kinase 4/6 inhibitor, preferentially inhibits proliferation of luminal estrogen receptor-positive human breast cancer cell lines in vitro. *Breast Cancer Res* 2009;11:R77.